Improvement of Power-Conversion Efficiency of a DC–DC Boost Converter Using a Passive Snubber Circuit

Jae-Jung Yun, Hyung-Jin Choe, Young-Ho Hwang, Yong-Kyu Park, and Bongkoo Kang, *Member, IEEE*

***Abstract*—This paper proposes a method of improving the power-conversion efficiency of a direct-current–direct-current boost converter. The proposed method uses a passive snubber circuit, which consists of two inductors, a capacitor, and a diode, to reduce switching loss. The proposed boost converter was built and tested on 42-, 47-, and 55-in edge-lit light-emitting-diode (LED) backlight units (BLUs). The power-conversion efficiency for an input voltage of 24 V was measured as 96%, 95.1%, and 93.7% for the 42-, 47-, and 55-in edge-lit LED BLUs, respectively; these values were 2.3%, 2.2%, and 2% higher than those of the conventional boost converters in the corresponding BLUs. The proposed boost converter ensured reliable operation and high-power efficiency under a ±10% variation of input voltage and a ±20% variation of the passive snubber component values.**

***Index Terms*—Direct-current–direct-current (dc–dc) power conversion, light-emitting-diode (LED) displays, snubbers.**

I. Introduction

A DIRECT-CURRENT–direct-current (dc–dc) boost converter is a step-up converter. It has several advantages over other step-up dc–dc converters. It has a simple structure that consists of a few components; therefore, it can easily be designed and implemented using a small inexpensive circuit. Various soft-switched boost converters with active or passive snubber circuits have been proposed [1]–[15]. Passive snubber circuits can achieve soft switching and reduce the reverse-recovery current of a rectifier diode by using only passive components such as inductors, capacitors, and diodes without auxiliary switches. Compared with active snubber circuits, passive snubber circuits are generally simpler to design and have fewer components; therefore, they are less expensive, more reliable, and smaller [7]–[15].

In this paper, a new high-efficiency dc–dc boost converter with a passive snubber circuit is proposed. The structure of the proposed circuit and its operation principles are described in Section II. The design considerations are given in Section III. The experimental results are given in Section IV, and a conclusion is given in Section V.

Manuscript received September 24, 2010; revised December 25, 2010, February 21, 2011, and March 23, 2011; accepted March 25, 2011. Date of publication April 7, 2011; date of current version November 1, 2011. This work was supported in part by the LG Display Company, Ltd. and in part by the Ministry of Education of Korea through the Brain Korea in the 21st Century Program.

J.-J. Yun, H.-J. Choe, and B. Kang are with the Department of Electrical Engineering, Pohang University of Science and Technology, Pohang 790-784, Korea (e-mail: jjyun@postech.ac.kr; hjchoe@postech.ac.kr; bkkang@ postech.ac.kr).

Y.-H. Hwang and Y.-K. Park are with the LG Display Company, Ltd., Liquid Crystal Display Division, Paju 413-811, Korea (e-mail: yhwang@lgdisplay.com; parkyongkyu@lgdisplay.com).

Digital Object Identifier 10.1109/TIE.2011.2141095

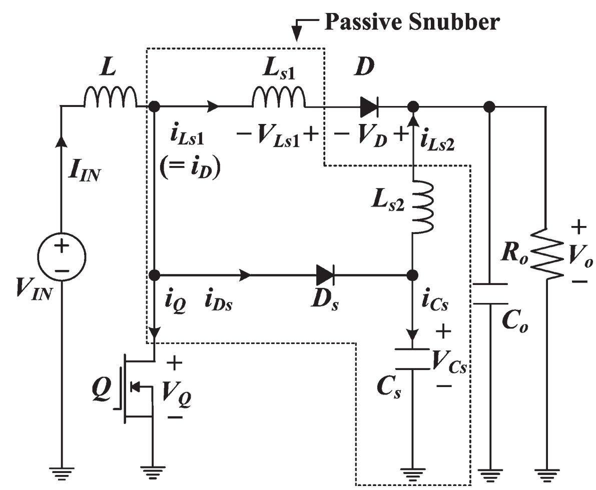

Fig. 1. Circuit diagram of the proposed boost converter. Its components are described in the text.

II. Proposed Circuit and Its Operation Principles

The proposed boost converter (see Fig. 1) has a passive snubber circuit consisting of capacitor C_s, diode D_s, and the two inductors L_{s1} and L_{s2}, in addition to the conventional boost converter consists of the boost inductor L, the boost switch Q, the boost diode D, and the output capacitor C_o. The inductances of L_{s1} and L_{s2} are much smaller than that of L, and the capacitance of C_s is much smaller than that of C_o.

The proposed boost converter uses a control pulse with the switching period T_s and the duty ratio D_r. It has five distinct operating modes during the switching period T_s, which result in the theoretical waveforms in Fig. 2. To simplify the analysis of operation, the inductance of L and the capacitance of C_o are assumed to be large enough that $V_{\rm IN}$ and L can be approximated as the constant current $I_{\rm IN}$ and that the voltage of C_o and R_o can be approximated as the constant voltage source V_O. In addition, L_{s1}, L_{s2}, and C_s are considered to be lossless, and the output capacitance and ON-state resistance of Q are neglected. Just before t_0, the following assumptions are made: Q is turned off, the voltage of C_s is $V_{C_s}(t_0)$, and the current of L_{s2} is $i_{L_{s2}}(t_0)$.

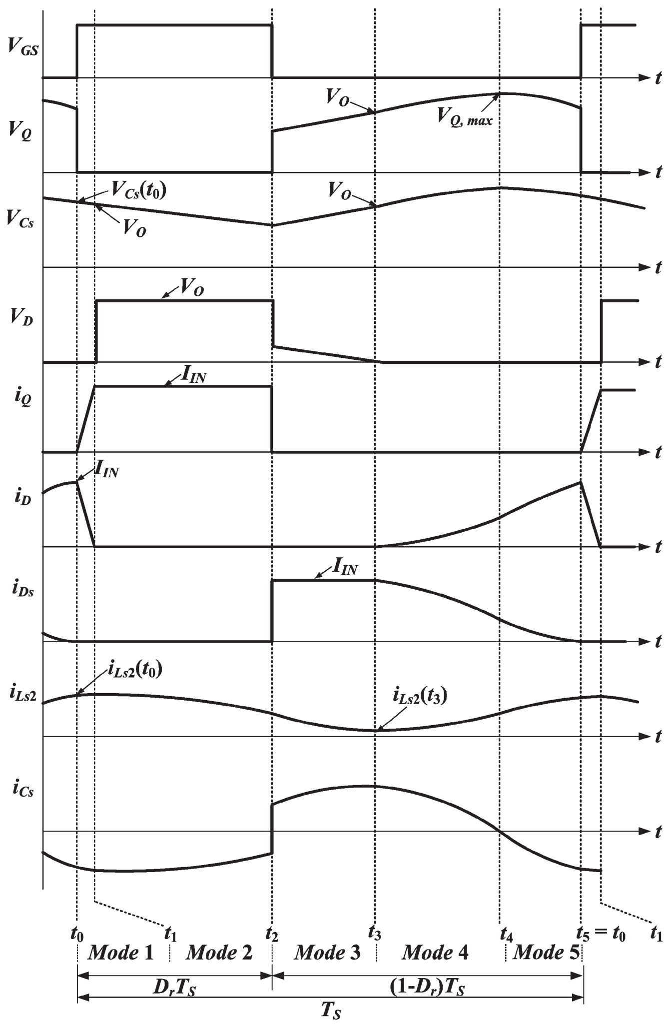

Fig. 2. Theoretical waveforms of the proposed boost converter.

Mode 1 $[t_0 - t_1]$*:* At t_0, Q is turned on, and current i_{D_s} has reached 0. Thus, D_s is turned off during this mode without any reverse-recovery process. i_D begins to decrease linearly because V_O applied across L_{s1} is constant, but i_Q begins to increase linearly at the same rate because $i_Q + i_D = I_{\rm IN}$, which is constant. Currents i_D and i_Q are given by

$$i_D(t) = I_{\rm IN} - \frac{V_O}{L_{s1}}(t - t_0)$$

$$i_Q(t) = \frac{V_O}{L_{s1}}(t - t_0).$$

Thus, Q is turned on at $t = t_0$ under zero-current switching (ZCS). i_D reaches 0, and i_Q reaches $I_{\rm IN}$ at

$$t = t_0 + \frac{I_{\rm IN} L_{s1}}{V_O} \equiv t_1.$$

During this mode, C_s is discharged through L_{s2} to the load by $i_{L_{s2}}$; thus, V_{C_s} decreases from $V_{C_s}\,(t_0)$ to V_O.

Mode 2 $[t_1 - t_2]$*:* In this mode, Q remains on, D_s remains off, and D is turned off without any reverse-recovery process because i_D has reached 0 at t_1; thus, $i_Q(t) = I_{\rm IN}$. At t_2, $i_{L_{s2}}$ reaches $i_{L_{s2}}\,(t_2)$, and V_{C_s} reaches $V_{C_s}(t_2)$.

Mode 3 $[t_2 - t_3]$*:* At t_2, Q is turned off, and D_s is turned on. D remains off. Thus, in this mode, $I_{\rm IN}$ flows through D_s. i_{D_s} $(= I_{\rm IN})$ is divided into $i_{L_{s2}}$ and i_{C_s}, which results in

$$\begin{aligned} i_{L_{s2}}(t) = &\frac{V_{C_s}(t_2) - V_O}{Z_1}\ \sin\,\omega_1(t - t_2) \\ &+ (i_{L_{s2}}(t_2) - I_{\rm IN})\ \cos\,\omega_1(t - t_2) + I_{\rm IN} \\ i_{C_s}(t) = &-\frac{V_{C_s}(t_2) - V_O}{Z_1}\ \sin\,\omega_1(t - t_2) \\ &- (i_{L_{s2}}(t_2) - I_{\rm IN})\ \cos\,\omega_1(t - t_2) \end{aligned}$$

where

$$\omega_1 = \frac{1}{\sqrt{L_{s2} C_s}} \quad Z_1 = \sqrt{\frac{L_{s2}}{C_s}}.$$

V_{C_s} increases slowly because C_s is charged by i_{C_s}. Because the forward voltage of D_s and the voltage across L_{s1} are negligibly small, $V_Q = V_{C_s}$, and $V_D = V_O - V_Q$. Thus, V_Q increases slowly, and V_D decreases slowly at the same rate, as given by

$$\begin{aligned} V_Q(t) =& (V_{C_s}(t_2) - V_O)\ \cos\,\omega_1(t - t_2) \\ &+ (I_{\rm IN} - i_{L_{s2}}(t_2))\, Z_1\ \sin\,\omega_1(t - t_2) + V_O \\ V_D(t) =& -(V_{C_s}(t_2) - V_O)\ \cos\,\omega_1(t - t_2) \\ &- (I_{\rm IN} - i_{L_{s2}}(t_2))\, Z_1\ \sin\,\omega_1(t - t_2). \end{aligned}$$

At t_3, V_Q increases to V_O. Thus, V_D decreases to 0, and D starts conducting. Currents $i_{L_{s2}}$ reaches $i_{L_{s2}}\,(t_3)$, and i_{C_s} reaches $i_{C_s}\,(t_3)$. The duration of this mode is

$$\Delta t_3 = t_3 - t_2 = \frac{1}{\omega_1}\ \tan^{-1}\left[\frac{V_O - V_{C_s}(t_2)}{(I_{\rm IN} - i_{L_{s2}}(t_2))\, Z_1}\right].$$

Mode 4 $[t_3 - t_4]$*:* In this mode, Q remains off, and D_s remains on. D is turned on at t_3, and i_D starts to increase slowly due to the resonance of L_{s1}, L_{s2}, and C_s. Thus, $I_{\rm IN}$ flows through D and D_s, and i_{D_s} is divided into $i_{L_{s2}}$ and i_{C_s}. Then, $i_{L_{s2}}$ flows through L_{s2} into V_O, and i_{C_s} charges C_s. V_Q $(= V_{C_s})$ is increased slowly from V_O by the resonant current i_{C_s}. V_Q, i_{C_s}, and $i_{L_{s2}}$ are given by

$$V_Q(t) = Z_2 i_{C_s}(t_3)\ \sin\,\omega_2(t - t_3) + V_O \tag{1}$$

$$\begin{aligned} i_{C_s}(t) =& i_{C_s}(t_3)\ \cos\,\omega_2(t - t_3) \\ i_{L_{s2}}(t) =& -\frac{L_{s1}}{L_{s1} + L_{s2}}\,(I_{\rm IN} - i_{L_{s2}}(t_3))\ \cos\,\omega_2(t - t_3) \\ &+ \frac{1}{L_{s1} + L_{s2}}\,(L_{s1} I_{\rm IN} + L_{s2} i_{L_{s2}}(t_3)) \end{aligned} \tag{2}$$

where

$$\omega_2 = \frac{1}{\sqrt{\frac{L_{s1} L_{s2}}{L_{s1} + L_{s2}} C_s}} Z_2 = \sqrt{\frac{L_{s1} L_{s2}}{(L_{s1} + L_{s2}) C_s}}.$$

By setting duration Δt_4 of this mode as

$$\Delta t_4 = t_4 - t_3 = \pi / 2\omega_2$$

i_{C_s} reaches 0; thus, Q has the maximum voltage $V_{Q,\max}$. From (1) and (2)

$$V_{Q,\max} = V_Q(t_4) = Z_2 i_{C_s}(t_3) + V_O. \tag{3}$$

In addition, $i_{L_{s2}}$ reaches $i_{L_{s2}}(t_4)$.

Mode 5 $[t_4 - t_5]$*:* In this mode, Q remains off, and D and D_s remain on. I_{IN} flows through the current paths $V_{\text{IN}} \rightarrow L_{s1} \rightarrow D \rightarrow V_O$ and $V_{\text{IN}} \rightarrow D_s \rightarrow L_{s2} \rightarrow V_O$, and i_{C_s} discharges C_s through the current path $C_s \rightarrow L_{s2} \rightarrow V_O$. V_Q $(= V_{C_s})$ is decreased from $V_{Q,\max}$ to $V_{C_s}(t_0)$ by i_{C_s}. V_Q, i_{C_s}, $i_{L_{s2}}$, and i_{D_s} are given by

$$\begin{aligned}
V_{C_s}(t) &= (V_{Q,\max} - V_O)\cos\omega_2(t-t_4) + V_O\\
i_{C_s}(t) &= -\frac{V_{Q,\max} - V_O}{Z_2}\sin\omega_2(t-t_4)\\
i_{L_{s2}}(t) &= i_{L_{s2}}(t_4) + \frac{(V_{Q,\max} - V_O)}{L_{s2}\omega_2}\sin\omega_2(t-t_4)\\
i_{D_s}(t) &= i_{L_{s2}}(t_4) + \left(\frac{1}{L_{s2}\omega_2} - \frac{1}{Z_2}\right)\\
&\quad\times (V_{Q,\max} - V_O)\sin\omega_2(t-t_4).
\end{aligned}$$

At t_5, i_{D_s} reaches 0, $i_{L_{s2}}$ reaches $i_{L_{s2}}(t_0)$, and V_{C_s} reaches $V_{C_s}(t_0)$. Duration Δt_5 of this mode is

$$\Delta t_5 = t_5 - t_4 = (1 - D_r)T_s - (\Delta t_4 + \Delta t_3).$$

Circuit operation is the same as in mode 1, when Q is turned on again at t_0 in the next switching cycle.

III. Design Considerations

In the proposed boost converter, the ZCS turning on of Q is achieved by controlling the turn-off di/dt of D using L_{s1} and eliminating the reverse-recovery current of D_s. L_{s1}, L_{s2}, and C_s are the main components that should be designed to achieve the optimal performance of the proposed boost converter. To control the turn-off di/dt of D, L_{s1} should be determined according to [7]

$$L_{s1} > \frac{V_O t_r}{I_{\text{IN}}} \equiv L_{s1,\min} \tag{4}$$

where the switch current rise time t_r is dictated by Q and its gate drive circuit. L_{s1} should be larger than $L_{s1,\min}$ to guarantee the ZCS turning on of Q. In practice, as L_{s1} increases, the switching loss decreases, but the inductor loss increases. Thus, L_{s1} should be determined experimentally so that the sum of the switching and inductor losses has the minimum value.

To eliminate the reverse-recovery current of D_s, current i_{D_s} should reach 0 at t_5. Thus, the following equations should be satisfied:

$$\begin{aligned}
1 &= \frac{L_{s2}}{L_{s1}+L_{s2}}\left(\cos\omega_1\Delta t_3 - \frac{\sin\omega_1\Delta t_3}{\tan\omega_1(\Delta t_2+\Delta t_3)}\right)\\
&\quad\times(1+\sin\omega_2\Delta t_5)\\
\Delta t_3 &= (1-D_r)T_s - \frac{\pi}{2\omega_2} - \frac{1}{\omega_2}\tan^{-1}\left(\frac{Z_2}{Z_1\tan\omega_1\Delta t_1}\right)\\
\Delta t_5 &= \frac{1}{\omega_2}\tan^{-1}\left(\frac{Z_2}{Z_1\tan\omega_1\Delta t_1}\right).
\end{aligned} \tag{5}$$

If $i_{D_s} > 0$ at t_5, switching losses occur at the instant of switch turn-on due to the high turn-off di/dt and the reverse-recovery current of D_s; if i_{D_s} reaches 0 at t_{D_s} $(t_4 < t_{D_s} < t_5)$, the parasitic oscillation of Q occurs due to the resonance of L_{s1} and the internal capacitance of Q during $t_{D_s} - t_5$ and causes extra power losses. However, these losses are smaller than the reverse-recovery-related loss of the boost diode in the conventional boost converter.

In the proposed boost converter, it is required that the input energy and the energy stored in C_s are transferred to the output load during the overall operating modes. Thus, $i_{L_{s2}}$ that has the minimum value at t_3 (in mode 3) should be

$$i_{L_{s2}}(t_3) = I_{\text{IN}}\left(1 - \cos\omega_1\Delta t_3 + \frac{\sin\omega_1\Delta t_3}{\tan\omega_1(\Delta t_2+\Delta t_3)}\right) > 0. \tag{6}$$

Otherwise, the energy stored in C_o is transferred to C_s while $i_{L_{s2}} < 0$.

The voltage stress of diodes D and D_s are determined by V_O, and the voltage stress of Q is determined by $V_{Q,\max}$, as given in (3). $V_{Q,\max}$ can be presented as

$$V_{Q,\max} = Z_2 I_{\text{IN}}\left(cos\omega_1\Delta t_3 - \frac{\sin\omega_1\Delta t_3}{\tan\omega_1(\Delta t_2+\Delta t_3)}\right) + V_O. \tag{7}$$

Due to the resonant peak generated by L_{s1}, L_{s2}, and C_s, the voltage stress $(= V_{Q,\max})$ of Q in the proposed boost converter is higher than $(= V_O)$ in the conventional boost converter. The current stress of Q, D, and D_s is determined by I_{IN}, and the current stress of Q in the proposed boost converter is lower than that in the conventional boost converter because the reverse-recovery-current spikes of D and D_s are eliminated in the proposed boost converter.

Although the circuit parameters could be determined using (4)–(7), it requires some iteration of parameter calculations. A simpler design guide would be obtained by observing the waveforms of V_{C_s} and $i_{L_{s2}}$ in Fig. 2. Conditions $V_{C_s}(t_5) > V_O$ and $i_{L_{s2}}(t_5) > i_{L_{s2}}(t_2)$ should to be satisfied to have a stable operation, which results in

$$\frac{\pi}{T_s}\left(\frac{1}{4\omega_1} + \frac{1}{2\omega_2}\right) < 1 - D_r < \frac{\pi}{T_s}\left(\frac{1}{4\omega_1} + \frac{1}{\omega_2}\right).$$

ω_1 needs to be small enough to satisfy $i_{C_s}(t_2) < 0$, which guarantees $i_{L_{s2}}(t_2) > 0$ and results in

$$D_{r,\max} - \frac{1}{T_S}\frac{I_{\text{IN}}L_{s1}}{V_O} < \frac{1}{T_S}\frac{\pi}{2\omega_1}.$$

IV. Experimental Results

For large-scale liquid-crystal-display televisions, light-emitting-diode (LED) backlight units (BLUs) are gradually replacing cold-cathode-fluorescent-lamp and external-electrode-fluorescent-lamp BLUs [16]–[23], which contain mercury and require a high-voltage power source [24], [25]. The step-up dc–dc converters are needed to provide sufficient voltage to overcome the high forward voltages of LED arrays for edge-lit LED BLUs. Therefore, the fabricated circuit of the proposed boost converter (see Fig. 3) was tested on 42-,

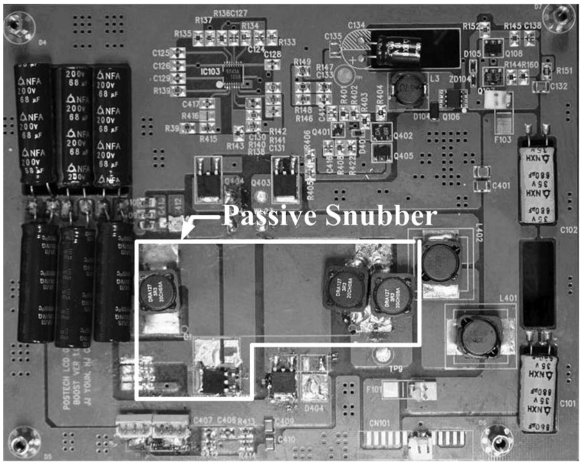

Fig. 3. Hardware circuit of the proposed boost converter.

47-, and 55-in edge-lit LED BLUs, which require the output power P_o of 73.5, 90, and 122.5 W, respectively. In addition, a conventional boost converter with the same specifications was built for comparison. To reduce electromagnetic interference noise generated at the instant of turn-off switching, simple resistance–capacitance snubber circuits composed of a resistor (10 Ω) and a capacitor (1 nF) were connected in parallel to the boost switches and diodes of the proposed and conventional boost converters. The boost converters were designed to produce the constant dc output $V_O = 35$ V for an input voltage V_{IN} range of 24 V $\pm$ 10%. They were operated at a switching frequency of 278 kHz. A dc voltage feedback control was used to ensure the stability of the converters. The circuits were built using the following components: $L = 44\ \mu$H; $C_o = 408\ \mu$F; BA9743AFV from Rohm Company, Ltd. for pulse width modulation; SUD40N10-25 from Vishay Inc. for switch Q; and SBR6100CTL from Diodes Inc. for diodes D and D_s.

The values of L_{s1}, L_{s2}, and C_s for the passive snubber circuit were determined using (4)–(7). The lowest I_{IN} value was 3.06 A, and the longest t_r value was ~110 ns for the intended application. $L_{s1,\min}$ was obtained as 1.26 μH using (4). A safety factor of 1.3 was multiplied to $L_{s1,\min}$ to obtain $L_{s1} = 1.65\ \mu$H. After determining L_{s1}, L_{s2} and C_s were determined using (5)–(7) such that $i_{D_s}(t_5) \approx 0$ A, $i_{L_{s2}}(t_3) > 0$ A, and $V_{Q,\max}$ was less than the desired $V_{Q,\max}$ value for the entire output power range. For the LED-BLU experiment, $L_{s2} = 3.3\ \mu$H, and $C_s = 320$ nF, which resulted in $V_{Q,\max} < 43$ V for $73 \le P_O \le 123$ W.

The current and voltage waveforms of switch Q were measured at $V_{\mathrm{IN}} = 24$ V, $V_O = 35$ V, and $P_O = 90$ W (see Fig. 4). The switch Q of the conventional boost converter switched under the hard switching conditions at the instant of turn-on and turn-off, and the turn-on loss was much larger than the turn-off loss for Q. The experimental switch waveforms of the proposed boost converter agreed with the theoretical waveforms in Fig. 2, except for the parasitic oscillations of V_Q and i_Q; Q was turned on under the ZCS condition, as discussed in mode 1.

The power efficiency values of the proposed and conventional boost converters were compared at $P_O = 73.5$, 90, and 122.5 W (see Fig. 5). The proposed one had higher power efficiency over the entire input voltage (24 V $\pm$ 10%) and load ranges (73.5, 90, and 122.5 W) than the conventional one. The measured power efficiency of the proposed one (and improvement over conventional one) with an input voltage of 24 V was 96% (2.3%) at $P_O = 73.5$ W, 95.1% (2.2%) at $P_O = 90$ W, and 93.7% (2%) at $P_O = 122.5$ W.

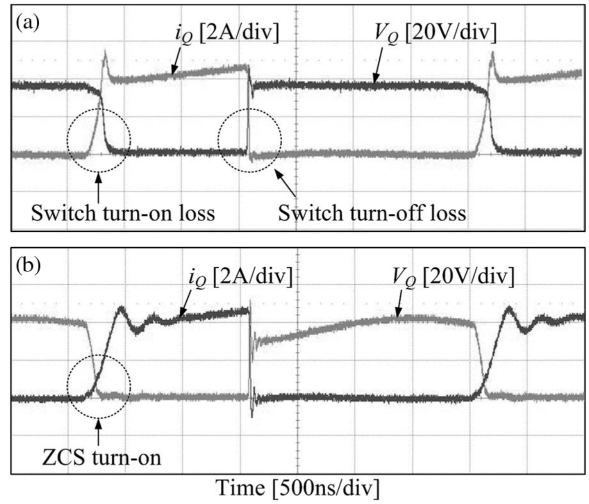

Fig. 4. Experimental current i_Q and voltage V_Q waveforms of switch Q at $V_{\mathrm{IN}} = 24$ V, $V_O = 35$ V, and $P_O = 90$ W: (a) conventional and (b) proposed boost converters.

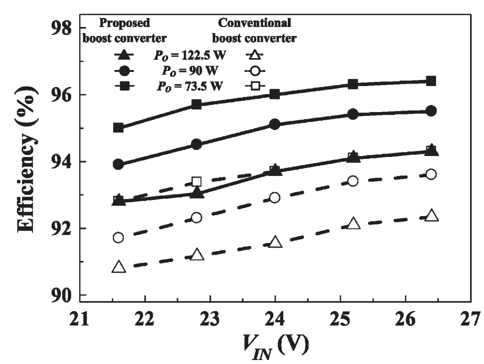

Fig. 5. Measured power efficiency versus V_{IN} (24 V $\pm$ 10%) for the proposed boost converter in comparison with the conventional boost converter at $P_O = 73.5$, 90, and 122.5 W.

The turn-on power loss P_Q of Q is given as

$$P_Q \approx f_s V_O [I_{\mathrm{IN}} t_r / 2 + Q_{\mathrm{rr}}] \tag{8}$$

where Q_{rr} and t_r are the reverse-recovery charge and the switch current rise time, respectively. The turn-on losses calculated by (8) were 1.56, 2.11, and 3.33 W for $P_O = 73.5, 90,$ and 122.5 W, respectively. The proposed boost converter reduces P_Q using the passive snubber circuit to improve the power efficiency.

The power efficiency of the proposed boost converter was measured at $V_{\mathrm{IN}} = 24$ V, $V_O = 35$ V, and $P_O = 73.5, 90,$ and 122.5 W while varying the circuit parameters L_{s1}, L_{s2}, and C_s by $\pm$ 20% from the designed values (see Fig. 6). It was highest at the designed values but was decreased by < 0.5% when the circuit parameters was changed by $\pm$20%.

At $V_{\mathrm{IN}} = 24$ V, $V_O = 35$ V, and $f_s = 278$ kHz, the electrical characteristics of the main components of the proposed boost

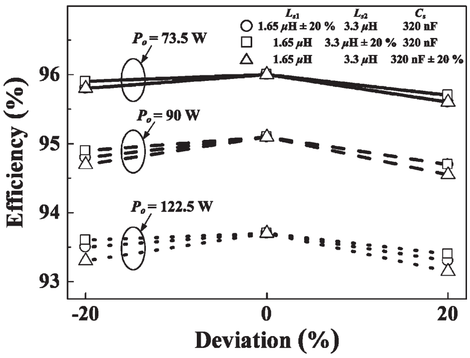

Fig. 6. Measured power efficiency for the proposed boost converter versus variation of circuit parameters from the designed values. Operating conditions: $V_{\mathrm{IN}} = 24$ V, $V_O = 35$ V, and $P_o = 73.5, 90,$ and 122.5 W.

TABLE I
ELECTRICAL CHARACTERISTICS OF THE MAIN COMPONENTS

		Proposed converter	Converter of [7]	Converter of [14]
Number of extra components		4	4	7
Efficiency (%)	42-inch	96 (97.1)	95.4 (96.7)	95.1 (97.1)
	47-inch	95.1 (97.1)	94.4 (96.7)	94.2 (97)
	55-inch	93.7 (97)	93.5 (96.4)	92.8 (96.8)
Peak switch voltage (V)	42-inch	40.2 (40.2)	84 (60.5)	64 (43.5)
	47-inch	41.7 (41.4)	85.5 (60.5)	76 (43.7)
	55-inch	43.6 (43.2)	87.3 (60.7)	93 (43.8)
Peak switch current (A)	42-inch	4.2 (3.7)	6 (5.9)	4.8 (4.2)
	47-inch	4.7 (4.4)	6.8 (6.6)	5.4 (4.9)
	55-inch	6.1 (5.7)	8 (7.8)	6.4 (5.8)
Peak diode reverse voltage (V)	42-inch	55 (60.5)	90 (90.2)	63.4 (59)
	47-inch	55.8 (60.7)	90 (90.5)	63 (60)
	55-inch	57 (60.5)	90 (90.5)	68 (59.1)

converter were compared with those of the two other previous ones in [7] and [14] using circuit simulations (see the values in parenthesis in Table I) and experimental circuits (see the values without parenthesis in Table I). All converters had nearly the same power efficiency values. The number of extra components is four for that in [7] and for the proposed one, whereas it is seven for that in [14]. Circuit simulations show that the proposed converter has peak switch voltages and currents, and peak diode reverse voltages close to that in [14] but much lower than that in [7]. The difference between the measured and simulated peak switch voltages is significant for the converters in [7] and [14], whereas it is negligibly small for the proposed one. The converters in [7] and [14] require two very tightly coupled inductors. Some leakage inductance increases switch turn-off loss and peak voltage. Considering that the proposed one had nearly the same performance for the ±20% variation of circuit parameters from the designed values (see Fig. 6), the proposed converter is more tolerant to circuit parameter variations than the others.

The power efficiency values of the proposed and conventional boost converters were measured at $P_o = 73.5, 90,$ and 122.5 W while varying the duty ratio D_d for the phase-shifted-pulsewidth-modulation dimming method [16] (see Fig. 7). For the entire D_d range and all load conditions, the proposed one had higher power efficiency than the conventional one. The difference of power efficiency between the proposed and conventional ones decreased from ~2.2% to 1.5% as D_d decreased from 100% to 20%.

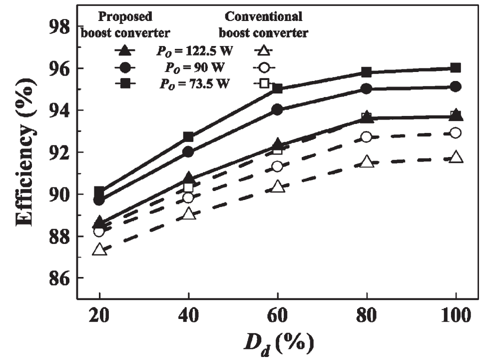

Fig. 7. Measured power efficiency versus D_d for the proposed boost converter in comparison with the conventional boost converter at $P_O = 73.5, 90,$ and 122.5 W.

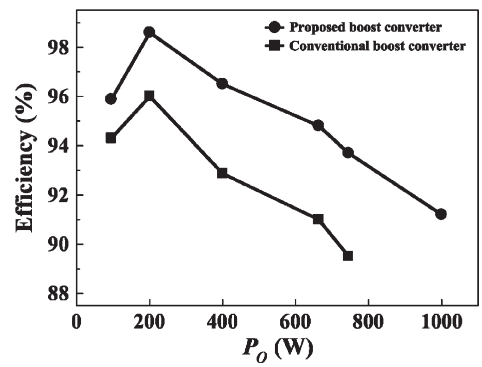

Fig. 8. Measured power efficiency versus P_O at $V_{\mathrm{IN}} = 85$ V, $V_O = 160$ V, and $f_s = 100$ kHz for the proposed boost converter in comparison with the conventional boost converter.

The change of power efficiency was measured at $V_{\mathrm{IN}} = 85$ V, $V_o = 160$ V, and $f_s = 100$ kHz while varying P_o from 75 to 1000 W (see Fig. 8). To handle high power for this paper, the switch was changed to IRGP4050 from IRF Company, and the diodes were changed to DSEI30-12A from IXYS Company. In addition, to satisfy the design rules discussed in Section III, the circuit parameters were changed to $L_{s1} = 20$ μH, $L_{s2} = 23.5$ μH, and $C_s = 300$ nF. For both proposed and conventional converters, the power efficiency decreased as P_o increased. However, the proposed one had better power efficiency than the conventional one by 1.7%–4.7% over the entire load range.

The power efficiency and D_r versus V_{IN} curves for the proposed and conventional boost converters were measured at $V_O = 400$ V, $f_s = 100$ kHz, and $P_O = 300$ W (see Fig. 9), which show one disadvantage of boost converters (see Fig. 9). The power-conversion efficiency of the proposed converter was higher than 92% for $D_r < 0.6$, but it decreased to 88% at $D_r = 0.66$. The conduction loss increased as D_r increased. Although the turn-on losses were reduced by the passive snubber circuit, the increased conduction loss caused the observed decrease

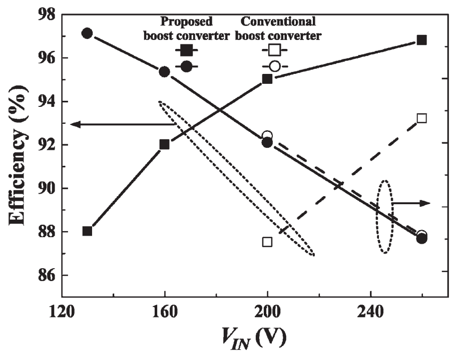

Fig. 9. Measured power efficiency and D_r versus V_{IN} for the proposed and conventional boost converters at $V_O = 400$ V, $f_s = 100$ kHz, and $P_O = 300$ W.

in power-conversion efficiency. Because of this problem, the proposed converter needs to operate at $D_r < 0.6$ to achieve high-power-conversion efficiency.

V. Conclusion

A new high-efficiency dc–dc boost converter with a passive snubber circuit is proposed. The passive snubber circuit consists of two inductors, a capacitor, and a diode; it reduces the reverse-recovery-related losses of the diodes and provides ZCS turn-on for the boost switch. The circuit of the proposed boost converter was built and tested on 42-, 47-, and 55-in edge-lit LED BLUs. The power efficiency of the proposed boost converter with the input voltage of 24 V was 96%, 95.1%, and 93.7% for 42-, 47-, and 55-in edge-lit LED BLUs; these were 2.3%, 2.2%, and 2% higher than those of the conventional boost converters in the corresponding BLUs. Compared with the conventional boost converter, the current stress and thermal stress of the boost switch and the diode were decreased, whereas the voltage stress of the boost switch and the diode was increased. In addition, the proposed boost converter ensured the reliable operation and high-power efficiency under the $\pm 10\%$ variation of the input voltage and $\pm 20\%$ variation of passive-snubber-component values.

References

[1] J. Bauman and M. Kazerani, "A novel capacitor-switched regenerative snubber for dc/dc boost converters," *IEEE Trans. Ind. Electron.*, vol. 58, no. 2, pp. 514–523, Feb. 2011.

[2] S.-H. Park, G.-R. Cha, Y.-C. Jung, and C.-Y. Won, "Design and application for PV generation system using a soft-switching boost converter with SARC," *IEEE Trans. Ind. Electron.*, vol. 57, no. 2, pp. 515–522, Feb. 2010.

[3] S.-H. Park, S.-R. Park, J.-S. Yu, Y.-C. Jung, and C.-Y. Won, "Analysis and design of a soft-switching boost converter with an HI-bridge auxiliary resonant circuit," *IEEE Trans. Power Electron.*, vol. 25, no. 8, pp. 2142–2149, Aug. 2010.

[4] S. Park and S. Choi, "Soft-switched CCM boost converters with high voltage gain for high-power applications," *IEEE Trans. Power Electron.*, vol. 25, no. 5, pp. 1211–1217, May 2010.

[5] H.-L. Do, "A soft-switching dc/dc converter with high voltage gain," *IEEE Trans. Power Electron.*, vol. 25, no. 5, pp. 1193–2010, May 2010.

[6] I. Aksoy, H. Bodur, and A. F. Bakan, "A new ZVT-ZCT-PWM dc–dc converter," *IEEE Trans. Power Electron.*, vol. 25, no. 8, pp. 2093–2105, Aug. 2010.

[7] M. R. Amini and H. Farzanehfard, "Novel family of PWM soft-single-switched dc–dc converters with coupled inductors," *IEEE Trans. Ind. Electron.*, vol. 56, no. 6, pp. 2108–2114, Jun. 2009.

[8] J. M. Kwon, W. Y. Choi, and B. H. Kwon, "Cost-effective boost converter with reverse-recovery reduction and power factor correction," *IEEE Trans. Ind. Electron.*, vol. 55, no. 1, pp. 471–473, Jan. 2008.

[9] R. H. Li, H. S. H. Chung, and A. T. Sung, "Passive lossless snubber for boost PFC with minimum voltage and current stress," *IEEE Trans. Power Electron.*, vol. 25, no. 3, pp. 602–613, Mar. 2010.

[10] R. J. Wai, C. Y. Lin, R. Y. Daun, and Y. R. Chang, "High-efficiency dc–dc converter with high voltage gain and reduced switch stress," *IEEE Trans. Ind. Electron.*, vol. 54, no. 1, pp. 354–364, Feb. 2007.

[11] C. A. Callo, F. L. Tofoli, and J. A. C. Pinto, "A passive lossless snubber applied to the ac–dc interleaved boost converter," *IEEE Trans. Power Electron.*, vol. 25, no. 3, pp. 775–785, Mar. 2010.

[12] R. J. Wai and R. Y. Daun, "High step-up converter with coupled-inductor," *IEEE Trans. Power Electron.*, vol. 20, no. 5, pp. 1025–1035, Sep. 2005.

[13] D. D. C. Lu, D. K. W. Cheng, and Y. S. Lee, "A single-switch continuous-conduction-mode boost converter with reduced reverse-recovery and switching losses," *IEEE Trans. Ind. Electron.*, vol. 50, no. 4, pp. 767–776, Aug. 2003.

[14] E. S. Silva, L. R. Barbosa, J. B. Vieira, Jr., L. C. Freitas, and V. J. Farias, "An improved boost PWM soft-single-switched converter with low voltage and current stresses," *IEEE Trans. Ind. Electron.*, vol. 48, no. 6, pp. 1174–1178, Dec. 2001.

[15] R. H. Li and H. S. Chung, "A passive lossless snubber cell with minimum stress and wide soft-switching range," *IEEE Trans. Power Electron.*, vol. 25, no. 7, pp. 1725–1738, Jul. 2010.

[16] Y. K. Lo, K. H. Wu, K. J. Pai, and H. J. Chiu, "Design and implementation of RGB LED drivers for LCD backlight modules," *IEEE Trans. Ind. Electron.*, vol. 56, no. 12, pp. 4862–4871, Dec. 2009.

[17] C. Y. Wu, T. F. Wu, J. R. Tsai, Y. M. Chen, and C. C. Chen, "Multistring LED backlight driving system for LCD panels with color sequential display and area control," *IEEE Trans. Ind. Electron.*, vol. 55, no. 10, pp. 3791–3800, Oct. 2008.

[18] H. J. Chiu and S. J. Cheng, "LED backlight driving system for large-scale LCD panels," *IEEE Trans. Ind. Electron.*, vol. 54, no. 5, pp. 2751–2760, Oct. 2007.

[19] C. C. Chen, C. Y. Wu, Y. M. Chen, and T. F. Wu, "Sequential color LED backlight driving system for LCD panels," *IEEE Trans. Power Electron.*, vol. 22, no. 3, pp. 919–925, May 2007.

[20] H.-J. Chiu, Y.-K. Lo, J.-T. Chen, S.-J. Cheng, C.-Y. Lin, and S.-C. Mou, "A high-efficiency dimmable LED driver for low-power lighting application," *IEEE Trans. Ind. Electron.*, vol. 57, no. 2, pp. 735–743, Feb. 2010.

[21] H. J. Chiu, Y. K. Lo, T. P. Lee, S. C. Mou, and H. M. Huang, "Design of an RGB LED backlight circuit for liquid crystal display panels," *IEEE Trans. Ind. Electron.*, vol. 56, no. 7, pp. 2793–2795, Jul. 2009.

[22] W. S. Oh, D. Cho, K. M. Cho, G. W. Moon, B. Yang, and T. Jang, "A novel two-dimensional adaptive dimming technique of X–Y channel drivers for LED backlight System in LCD TVs," *J. Display Technol.*, vol. 5, no. 1, pp. 20–26, Jan. 2009.

[23] C. Y. Hsieh and K. H. Chen, "Boost dc–dc converter with fast reference tracking (FRT) and charge-recycling (CR) techniques for high-efficiency and low-cost LED driver," *IEEE J. Solid-State Circuits*, vol. 44, no. 9, pp. 2568–2580, Sep. 2009.

[24] Y. H. Liu, "Design and implementation of an FPGA-based CCFL driving system with digital dimming capability," *IEEE Trans. Ind. Electron.*, vol. 54, no. 6, pp. 3307–3316, Dec. 2007.

[25] H.-C. Yen, "Analysis of balancing driver for multiple cold cathode fluorescent lamps," *IEEE Trans. Ind. Electron.*, vol. 57, no. 4, pp. 1354–1359, Apr. 2010.

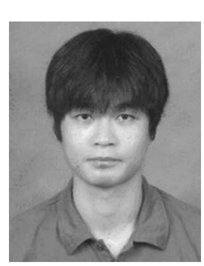

Jae-Jung Yun received the B.S. degree in electrical engineering from Hanyang University, Seoul, Korea, in 2006 and the M.S. degree in electrical engineering from Pohang University of Science and Technology, Pohang, Korea, in 2008, where he is currently working toward the Ph.D. degree in electrical engineering.

His research interests include the design and control of power converters, and soft-switching power converters.

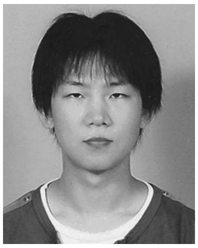

Hyung-Jin Choe received the B.S. degree in electrical engineering from Chungnam National University, Daejeon, Korea, in 2009 and the M.S. degree in electrical engineering from Pohang University of Science and Technology, Pohang, Korea, in 2011, where he is currently working toward the Ph.D. degree in electrical engineering.

His research interests include direct-current (dc)/dc and alternating-current/dc converters and light-emitting-diode driving systems.

Young-Ho Hwang received the B.S. degree in electrical engineering from Kwangwoon University, Seoul, Korea, in 2007 and the M.S. degree in electrical engineering from Pohang University of Science and Technology, Pohang, Korea, in 2009.

He is currently an Engineer with the Liquid Crystal Display Division, LG Display Company, Paju, Korea. His research interests include driving systems for light-emitting-diode backlights.

Yong-Kyu Park received the B.S. degree in electrical engineering from Hongik University, Seoul, Korea, in 2004 and the M.S. degree in electrical engineering from Pohang University of Science and Technology, Pohang, Korea, in 2006.

He is currently an Engineer with the Liquid Crystal Display Division, LG Display Company, Ltd., Paju, Korea. His research interests include driving systems for light-emitting-diode backlights.

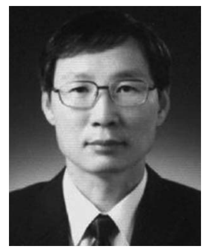

Bongkoo Kang (S'83–M'86) received the Ph.D. degree in electrical engineering from the University of California Berkeley, Berkeley, in 1986.

Following his graduation, he joined the Electronics and Telecommunication Research Laboratory, Taejeon, Korea, where he worked on developing semiconductor processing equipment. Since 1989, he has been a Professor with the Department of Electrical Engineering, Pohang University of Science and Technology, Pohang, Korea. His current research interests include the design of drive circuits for display devices and the modeling and characterization of semiconductor devices.